

# From ( $g2e$ ) to ( $geR$ ): kinematically complete experiments with COLTRIMS

T. Vogt<sup>1</sup>, R. Dörner<sup>1</sup>, O. Jagutzki<sup>1</sup>, C.L. Cocke<sup>2</sup>, J. Feagin<sup>3</sup>, M. Jung<sup>4</sup>, E.P. Kanter<sup>4</sup>, H. Khemliche<sup>5</sup>, S. Kravis<sup>2</sup>, V. Mergel<sup>1</sup>, L. Spielberger<sup>1</sup>, J.Ullrich<sup>6</sup>, M. Unverzagt<sup>1</sup>, U. Meyer<sup>1</sup> and H. Schmidt-Böcking<sup>1</sup>

<sup>1</sup> *Institut für Kernphysik, Universität Frankfurt, August-Euler-Str. 6, D-60486 Frankfurt, FRG*

<sup>2</sup> *J.R. McDonald Laboratory, Kansas State University., Manhattan, KS 66506, USA*

<sup>3</sup> *Dept. of Physics, California State Univ.-Fullerton, Fullerton, CA 92634, USA*

<sup>4</sup> *Argonne National Laboratory, Argonne, IL 60439, USA*

<sup>5</sup> *Lawrence Berkeley National Laboratory, Berkeley, CA 94720, USA*

<sup>6</sup> *Gesellschaft für Schwerionenforschung, D64291 Darmstadt, FRG*

We have applied the Cold Target Recoil Ion Momentum Spectroscopy (COLTRIMS) in combination with a large solid angle electron detector to investigate the complete momentum balance of He double photo-ionization at energies from 1 eV above threshold to 160 eV photon energy. We present triple differential cross sections  $d^3\sigma/d\Omega_1 d\Omega_2 dE$  deduced from these data and compare those with theory. For very low excess energy (Wannier regime) our experimental method accomplishes full detection solid angle for both the recoil ion and one emitted electron. Presenting the data Jacoby Coordinates it is thus possible to directly visualize the break-up of the atom. Recent calculations show very good agreement with our data.

## 1. Introduction:

The technique of Cold Target Recoil Ion Momentum Spectroscopy (COLTRIMS) has been developed to study the reaction dynamics in atomic collisions [1,2]. Recently this method has been applied to collisions of electrons and photons with helium [3,4,5,6,7]. Combining this technique with position sensitive large solid angle electron time-of-flight detectors it became possible to perform experiments of the type ( $e,2e$ ) [8] and ( $\gamma,2e$ ), with the recoil-ion momentum measurement replacing the spectroscopy of one electron.

In this paper we report on such kinematically complete experiments of the helium double photo-ionization at energies between 80 eV and 160 eV that were performed using COLTRIMS. These data can be compared to and expressed in triple differential cross sections  $d^3\sigma/d\Omega_1 d\Omega_2 dE$  (TDCS) such as obtained by the common ( $\gamma,2e$ )-technique with a pair of electrostatic electron spectrometers.

The first results on kinematically complete double photo-ionization measurements on helium target were reported by Schwarzkopf *et al.* [9] (see fig. 1) and have attracted considerable interest on theoretical [10,11,12,13] and experimental [14,15,16,17] side. Although the experimental setups have been improved since then, the ( $\gamma,2e$ ) technique with standard electron spectrometers generally suffers from

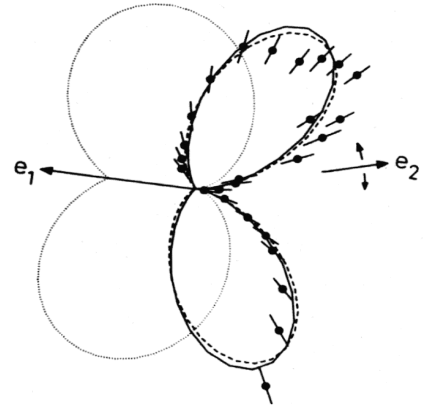


Figure 1:  
First experimental TDCS for ( $g2e$ )  
from Schwarzkopf *et al.* [9]

very small detection efficiency. This results in data with less statistical significance and only for selected kinematical conditions in the  $\Omega_1$ - $\Omega_2$ - $E$  hypersphere. However, the combined theoretical and experimental efforts already resulted in considerable progress in the field of electron-electron correlation.

The COLTRIMS-technique has the advantage that at threshold energy the combined geometrical detection solid angle can reach  $4\pi$  for *all* emitted particles. Even for higher energy the electron detection solid angle is still about  $1\pi$  while for the recoil ions always the whole momentum sphere ( $4\pi$ ) is measured. Furthermore, there are almost no apparatusive restrictions (none at all in the Wannier regime) on energy and angular configurations to be investigated and the statistical significance of the measured cross section distributions is much larger due the large solid detection angle without considerable loss of momentum resolution.

We present triple differential cross sections for double photo-ionization of helium acquired with this technique for photon energies of 1eV above threshold (Wannier regime) and for 120 eV and compare those with theory.

## 2. Experimental Setup

The use of cold target recoil ion momentum spectroscopy (COLTRIMS) in ion-He, electron-He and photon-He collisions is now well established [3,5,18]. The key feature of this method is that the He target is cooled in a supersonic expansion (gas jet) to an internal temperature well below 1 Kelvin such that the internal thermal momentum spread is below 0.05 a.u. which is much smaller than the momentum transfers of interests in typical atomic collisions ( $\approx 1$  a.u.). In the version of the apparatus we have used for the present studies the cooled gas jet was crossed by the photon beams of HASYLAB at DESY in Hamburg ( $E_\gamma = 120$  eV, 150 eV) and from the Advanced Light Source at the LBNL in Berkeley ( $E_\gamma = 80$  eV, 85 eV, 100 eV, 160 eV), respectively. The interaction zone is located in a well defined weak ( $\approx 1$ V/cm) electrostatic field region thus that recoil ions produced in the collisions are extracted onto a two-dimensional position sensitive multi-channel plate detector (see figure 2). The storage rings were operated in bunch modes that allowed to measure the time-of-flight of the recoil ions with the precision of less than a nanosecond. The momentum vector of the helium ions was determined from the measured time-of-flight and the position of the ion impinging on the detector. Note, that the complete momentum sphere of the recoil ions is measured simultaneously ( $4\pi$  solid angle) with a resolution of 0.1 a.u. for each momentum component and that single and double ionization events are distinct in time-of-flight.

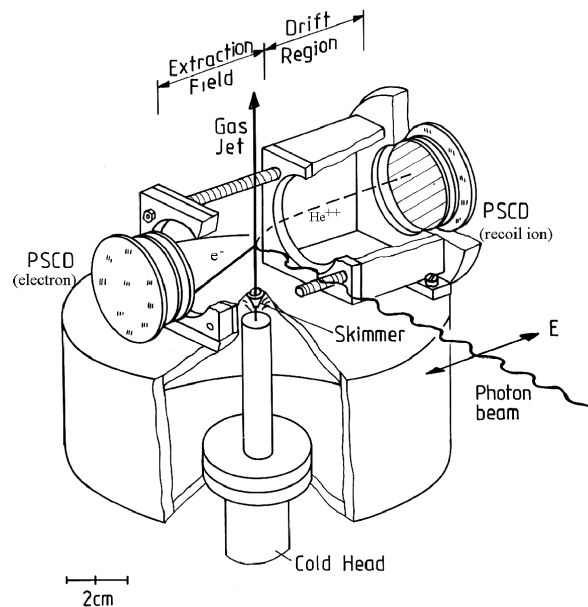


Figure 2:  
Sketch of the combined recoil-ion/electron momentum spectrometer

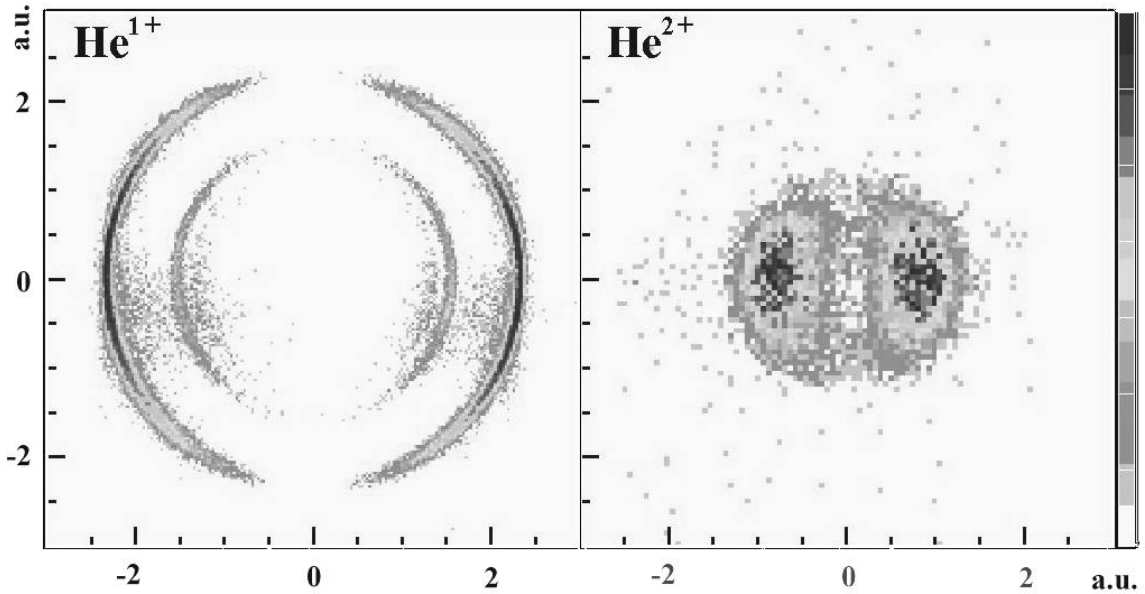


Figure 3:  
Density plots of the recoil ion momentum distributions for helium single (a) and double (b) photo-ionization for 150 eV photon energy in the plane perpendicular to the photon direction  $z$ . Only events are plotted with  $|\frac{1}{2}p_z| \leq 0.1$  a.u.

Figure 3 shows density plots of recoil ion momentum distributions for He single (a) and double (b) photo-ionization at  $E_\gamma = 150$  eV in the plane perpendicular to the photon beam direction ( $z$ -direction). Only events for a small  $z$ -momentum window of  $\pm 0.1$  a.u. are projected onto the  $x$ - $y$ -plane. For single ionization the distinct pattern of a dipole emission is visible. Since the recoil ion has to compensate the photo-electron momentum (the initial photon momentum can be neglected) the recoil ions have the same emission pattern in momentum space as the photo-electrons. The second structure in the center of fig. 3a arises from simultaneous excitation of the residual bound electron, thus reducing the released kinetic energy in the process. For double ionization this pattern changes since the second electron also carries momentum in this three-body process. However, a dipole-like emission pattern of the recoil ion is maintained.

A second position sensitive multi-channel plate detector facing the target region but located opposite to the ion detector detected one of the photo-electrons in coincidence with the ion. Events in which both electrons struck the detector could be rejected analyzing the pulse height distribution of the electron detector. The photo-electron momentum vector could be determined in the same way as for the recoiling ion. Up to 1 eV excess energy one of the photo-electrons could always be collected by the electrical field with  $4\pi$  solid angle. For higher energies (as  $E_\gamma = 120$  eV) so far only the geometrical detector area could be achieved as electron detection solid angle ( $\approx 1\pi$ ) since high energetic electrons not emitted into the direction of the active detector area escape from the weak electric field region in the spectrometer. However, the detection efficiency is still orders of magnitude bigger than for standard electron spectrometers and the orientation of the spectrometer was such that the polarisation vector of the mainly linearly polarized light pointed in the direction of the electron detector. Due to the dipole emission pattern of the electrons that dominates even for double ionization events at these higher energies [19], most of the interesting emission pattern can still be recorded.

The investigation of single ionization gave an excellent method to check the combined recoil ion/electron spectrometer system since electron and ion must show opposite momenta for each recorded single ionization event (the initial photon momentum is neglectable).

### 3. Triple differential cross sections for double photo-ionization of He

By coincident detection of all three momentum components of both recoil ion *and* one photo-electron the momentum balance of the double photo-ionization is completely determined, even overdetermined by one coordinate. We directly measure cross sections<sup>1</sup>  $d^2\sigma/d\mathbf{k}_{\text{rec}}d\mathbf{k}_e$  differential in the recoil ion momentum vector  $\mathbf{k}_{\text{rec}}$  and one electron momentum vector  $\mathbf{k}_e$ , with only 5 of the 6 variables being independent. In order to compare the data with the usual TDCS notation in spherical coordinates as function of the electron emission angles and their energy sharing the measured data were transformed using simple algebra and momentum conservation

$$\mathbf{k}_{e1} + \mathbf{k}_{e2} + \mathbf{k}_{\text{rec}} = \mathbf{k}_g (\cong \mathbf{0})$$

The energy conservation law

$$E_\gamma - E_{e1} - E_{e2} = E_{\text{rec}} (\cong 0)$$

was not used in the transformation but gave another possibility to check the data due to the redundancy of the measuring technique.

Being restricted in momentum space only by the electron solid detection angle it is now possible to slice the momentum sphere in angular „cake pieces“ and energy-share bins to derive cross section images as in figure 1. I.e., the five-dimensional cross sections are projected onto two-dimensional planes, e.g., for angle/energy combinations suggested by the cross section distribution's symmetries.

The general shape of the TDCS in fig. 1 can be explained by simple selection rules [10]. The TDCS must be zero for  $\mathbf{k}_{e1} = \mathbf{k}_{e2}$  due to the electron's repulsive Coulomb force. Final states with  $\mathbf{k}_{e1} = -\mathbf{k}_{e2}$  are forbidden because of parity violation. More exclusion principle exist for equal energy sharing and special angular configurations that result from the parity and/or angular momentum conservation laws. This can be seen in figure 4 where we present data obtained with our technique and transformed into TDCS for 41 eV excess energy and equal energy sharing. The angle  $\alpha$  between the polarization vector  $\mathbf{e}$  and one electron was fixed at three different angles ( $\alpha_{e1}$ )

and the TDCS as function of the second electron's angle  $\alpha_{e2}$  was plotted for planar geometry, i.e., only electrons in a narrow angular segment  $\Delta\beta$  in the plane perpendicular to the beam direction are considered. This corresponds to a ge-

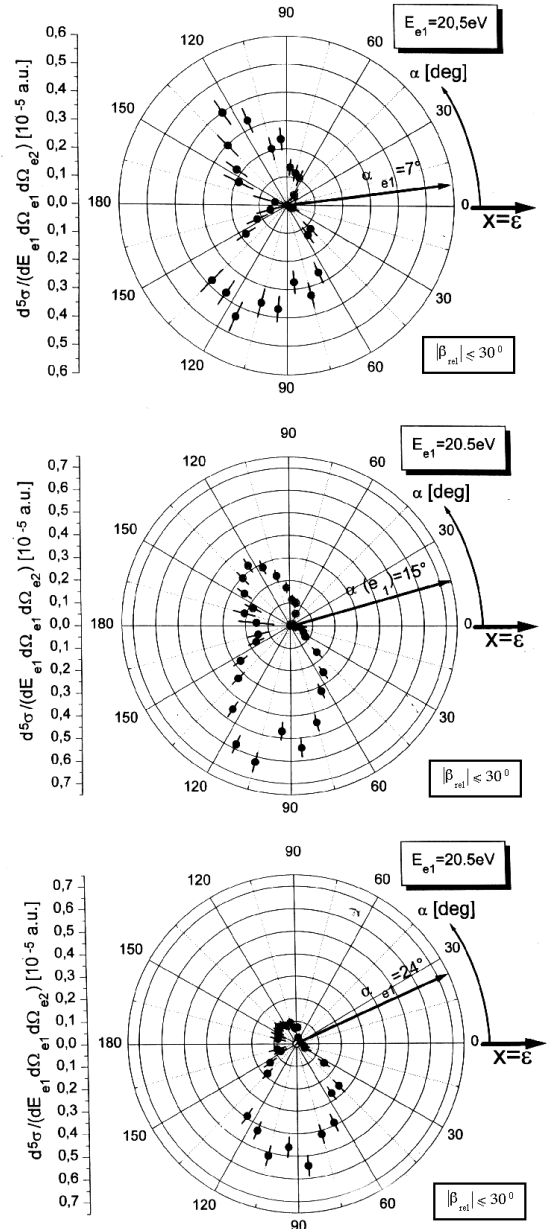


Figure 4: TDCS for planar geometry and equal energy sharing, for details see text

<sup>1</sup>Note that this cross section notation really represents a five-fold differential cross section as the TDCS is, too.

ometry that was chosen so far in the earlier  $(\gamma,2e)$ -measurements by setting the spectrometer's rotation axes and energy passes.

It is to note, that for obtaining these selected TDCS „views“ from our data we had to introduce the respective kinematical conditions by software, i.e., we performed „projections“ from our data set. Thus, all projections shown here are derived from only one single (and almost complete) five-dimensional data set, numerous other projection are possible.

The shrinking of the upper loop in fig.4 for increasing  $\alpha_{e1}$  from 0 towards  $30^\circ$  is in qualitative agreement with findings of Maulbetsch and Briggs [10], however, there are so far no calculations for  $E_\gamma=120$  eV and the experimental resolution and a non-perfect linear polarization of the beam do not yet allow stringent tests of theory.

Another „projection“ obtained from our data shows in figure 5 TDCS for fixed angle  $\alpha_{e1}$  but varying energy sharing between both electrons. Again, theory [10] seems to describe the main feature of the TDCS correctly although here, too, the chosen energy/angle parameters in the calculation are not exactly the same as in this experiment.

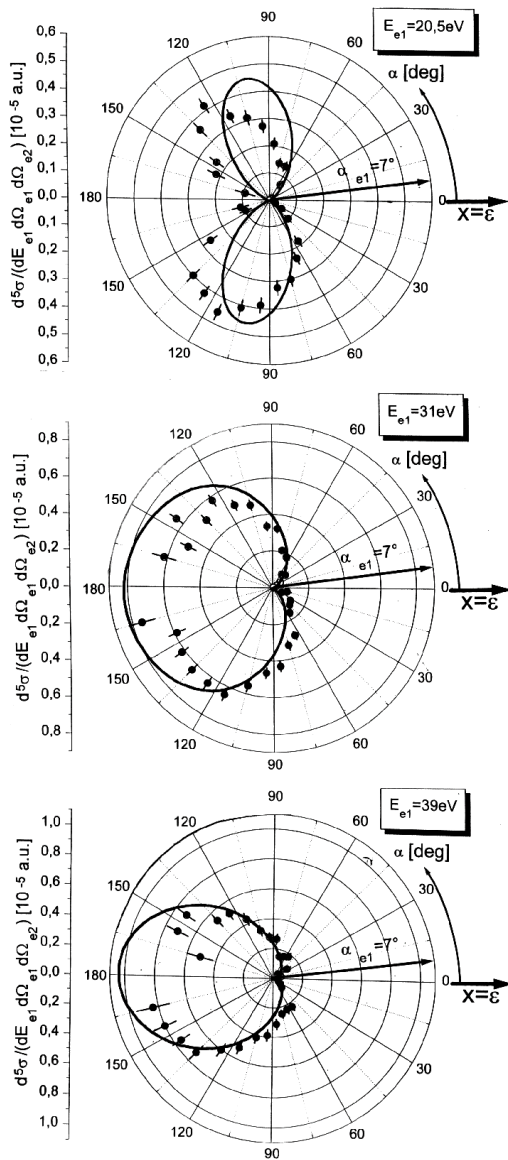


Figure 5:  
TDCS for unequal energy sharing. The solid lines show 3C-calculations of Maulbetsch and Briggs [10]

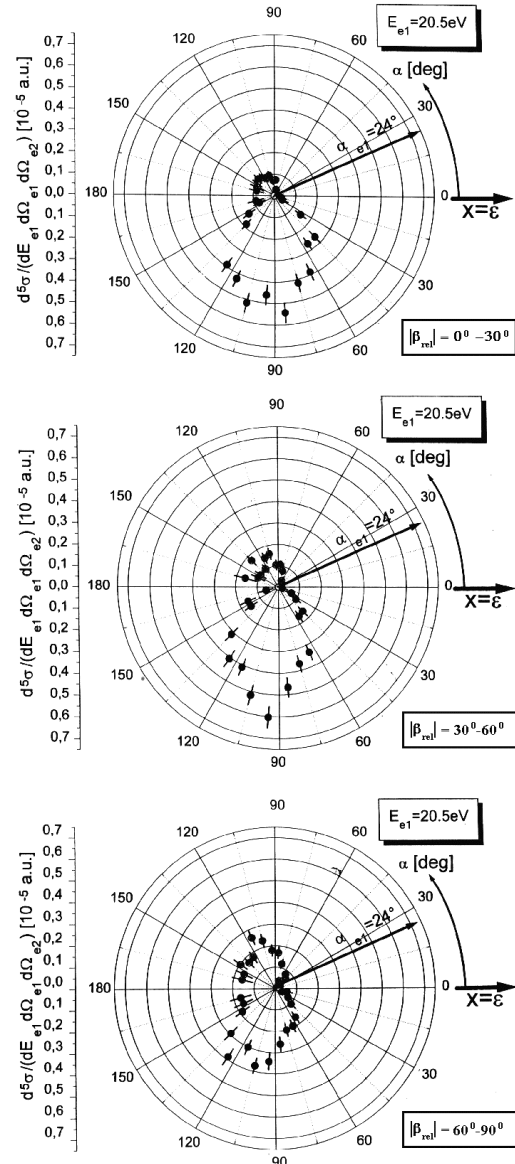


Figure 6:  
TDCS for equal energy sharing and „out-of-plane“ geometry. For details see text.

As stated earlier, almost any 2D-projection, i.e., choice of some fixed  $E$  -,  $\beta$  -,  $\alpha$  - combinations, for a TDCS presentation can be done, even out-of-plane geometries. In figure 6 the „observation angle“  $\beta_{e2}$  for the second electron is tilted out of the plane normal to the beam direction which is in contrast to the earlier in-plane figures. Again, calculations for such geometries exist already [10], but for a detailed check of the theoretical exclusion rules and analysis for the *physics* behind all those TDCS loops, it still requires smaller angular and energy resolution bins with sufficient statistics than were achievable in our first experiment and also „cleaner“ polarization features of the photon beam.

#### 4. Cross section representation in Jakoby Coordinates

For our experiments on the double photo-ionization at 1 eV excess energy we were able to measure the momenta of both the recoil ion and one electron with  $4\pi$  solid angle. Covering the complete momentum space enables us to formulate the cross sections in a different coordinate system that intertwines the measured momenta of recoil ion and electron. We propose the use of Jakoby Coordinates

$$\mathbf{k}_r = (\mathbf{k}_1 + \mathbf{k}_2) \quad \text{and} \quad \mathbf{k}_R = \frac{1}{2} (\mathbf{k}_1 - \mathbf{k}_2).$$

$\mathbf{k}_r$  describes the motion of the center-of-mass of the two electrons,  $\mathbf{k}_R$  the relative motion of the electrons. The introduction of this coordinate system has several advantages. It is used in the theoretical description of the Wannier process [20] but it is also the „natural“ coordinate system for our experimental method as the common TDCS-description suits the use of standard electron spectrometers. The value  $\mathbf{k}_r$  is directly accessible in our measurement since  $\mathbf{k}_r = -\mathbf{k}_{\text{rec}}$  (with  $\mathbf{k}_g \cong \mathbf{0}$ ). In this frame the kinematics of the Wannier process directly can be directly visualized [7]. Fig. 7 shows density plots of momentum distributions for the electron's center-of-mass (or recoil ion) motion (a), for a single electron (b) and for the relative electron motion (c) in the plane perpendicular to the photon beam direction, for details see figure caption. From this plot it is visible in a very intuitive way that the recoil ion emerges into the direction of the polarization vector of the linearly polarized light while the two electrons separate along a line perpendicular to that direction with their center of mass moving opposite to the recoil ion. Figure 8c shows another „view“ on the break-up process. Here the plane is perpendicular to the polarization vector direction. The relative-motion distribution forms a doughnut around the polarization axis as the electrons separate perpendicular to the polarization axis but the distribution is symmetrical around this axis.

For energies higher than 1 eV above threshold a complete detection of all electron momenta was not ensured with the present experimental setup to allow such a coordinate transformation in both  $\mathbf{k}_r$  and  $\mathbf{k}_R$ .

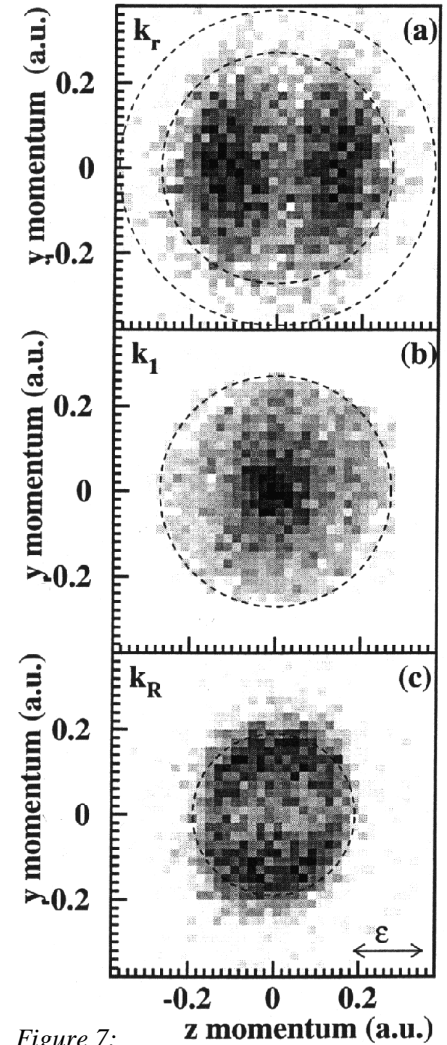


Figure 7: Density plots of projections of the momentum spectra in the plane perpendicular to the beam direction. Only events with  $|k_{rx}| \leq 0.01$  a.u. are plotted. The circles indicate the maximum possible values [7].

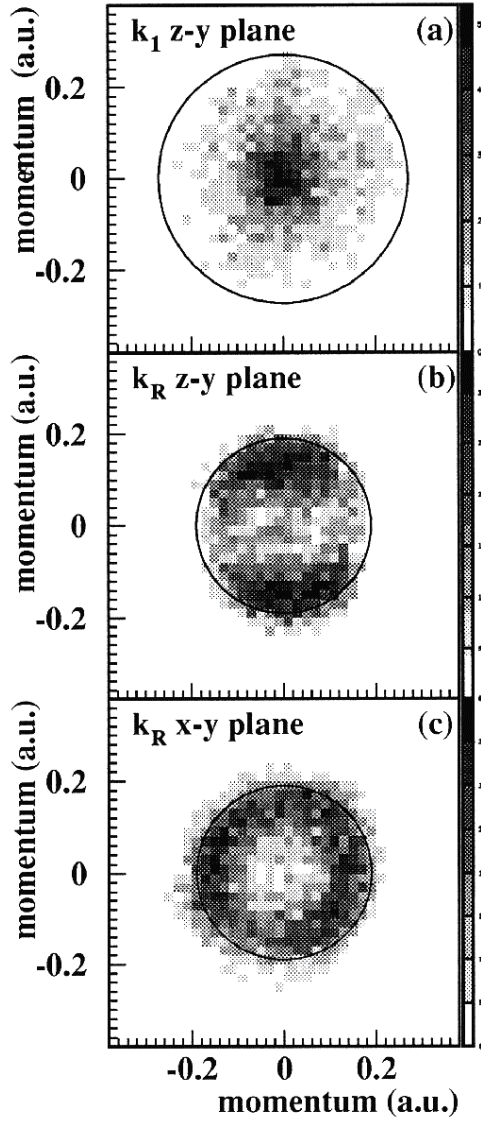


Figure 8:  
As figure 7, in (c) the relative electron momentum distribution is plotted in the plane perpendicular to the polarization vector direction.

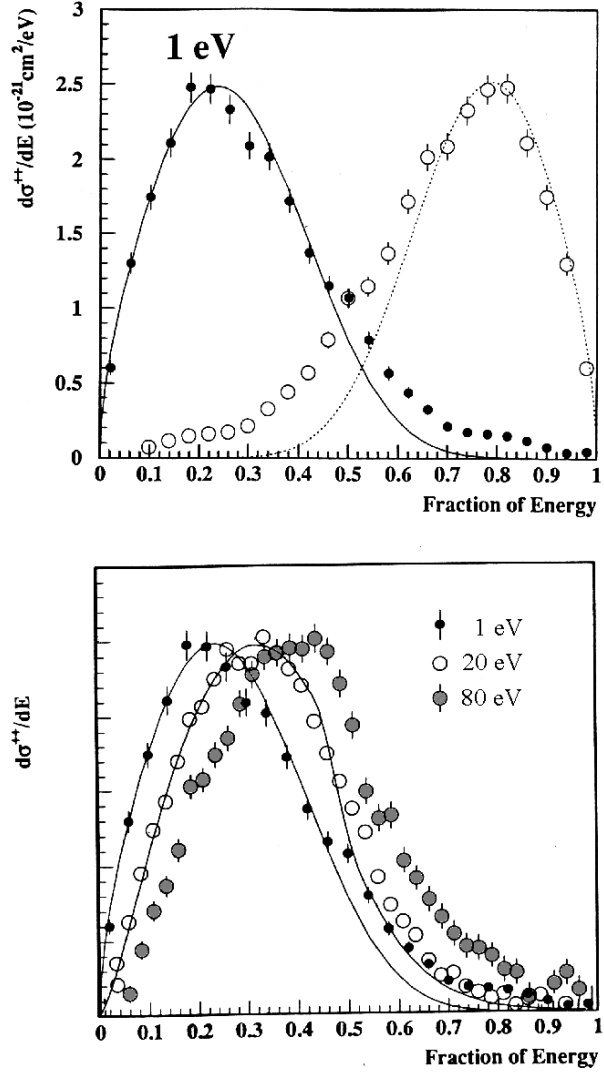


Figure 9:  
Fractions of kinetic energy deposited in the electron's relative motion and center-of-mass motion (a)  
Fraction of energy in the relative motion for different photon energies (b). For details see text.

However, since we always achieve  $4\pi$  momentum detection for the recoil ion momentum (and such for  $\mathbf{k}_r$ ) we can already compare all measured cross section distributions (for all photon energies investigated) as function of  $\mathbf{k}_r$ . In fig. 9a the relative portion of the energy deposited into the electron's center of mass motion and into the relative motion of both electrons is shown. For 1 eV excess energy most kinetic energy is found in the relative electron motion which is perfect agreement with the Wannier model. The line shows a calculation from Feagin in fourth-order Wannier theory [21] that fits the experimental results nicely [22].

At 20 eV excess energy the relative fraction of energy in the center-of-mass motion increases (see fig. 9b) which is also in perfect agreement on absolute scale with ab initio 2C calculations of Pont and Shakeshaft [23]. This energy portion in the center-of-mass motion seems to increase further towards equilibrium in the high energy regime where one electron carries almost all the kinetic energy (shake-off limit).

## 5. Summary and outlook:

We have measured the complete momentum balance after helium double photo-ionization at energies 1 eV above threshold and higher with the COLTRIMS technique. The data sets are complete in the sense that the momenta for all outgoing particles can be deduced for each event and almost the full detection solid angles for the particles could be achieved, at least for the Wannier regime. We can derive TDCS from our data without restrictions to any angular emission or energy sharing of the electrons. We propose the use of a cross section description in Jakoby Coordinates as the „natural frame“ of this atomic break-up process at low excess energies. The experimentally derived cross sections seem to be in good agreement with theory. Further experiments and fine-tuned theoretical analysis might reveal a better understanding of the underlying physical processes, such as electron-electron correlation, for the different TDCS. Investigations at higher energies are desirable to probe electron-electron correlation in the initial state, i.e., in the helium atom itself. We hope to improve our spectrometer system in the electron detection device to enable the full solid electron detection angle also for higher photon energies in the next future [24]. Furthermore, we design (e,3e)-like experiments applying the COLTRIMS technique [25].

## References:

1. J. Ullrich *et al.*, *Comm. At. Mol. Phys.* **30** (1994) 285
2. L. Spielberger *et al.*, *Nato ASI Series* **C414** (1993) 119
3. O. Jagutzki *et al.*, *Z. Phys.* **D36** (1996) 5
4. L. Spielberger *et al.*, *Phys. Rev. Lett.* **74** (1995) 4615
5. R. Dörner *et al.*, *Phys. Rev. Lett.* **76** (1996) 2654
6. L. Spielberger *et al.*, *Phys. Rev. Lett.* **76** (1996) 4685
7. R. Dörner *et al.*, *Phys. Rev. Lett.* **77** (1996) 1024
8. A. Kounis, diploma thesis (1996), in progress, not published
9. O. Schwarzkopf *et al.*, *Phys. Rev. Lett.* **70** (1993) 3008
10. F. Maulbetsch and J.S. Briggs, *Phys. Rev. Lett.* **68** (1992) 2004  
*J. Phys.* **B26** (1993) 1679  
*J. Phys.* **B26** (1993) L647  
*J. Phys.* **B27** (1994) 4095  
*J. Phys.* **B28** (1995) 551
11. M. Pont *et al.*, *Phys. Rev.* **A53** (1996) 3671
12. S.C. Ceraulo *et al.*, *Phys. Rev.* **A49** (1994) 1730
13. G. Dawber *et al.*, *J. Phys.* **B28** (1995) L271
14. A. Huetz *et al.*, *J. Phys.* **B27** (1994) L13
15. O. Schwarzkopf *et al.*, *J. Phys.* **B27** (1994) L347
16. P. Lablanquie *et al.*, *Phys. Rev. Lett.* **74** (1995) 2192
17. O. Schwarzkopf and V. Schmidt, *J. Phys.* **B28** (1995) 2847
18. R. Moshhammer *et al.*, *Phys. Rev. Lett.* **73** (1994) 3371  
*Phys. Rev. Lett.* **77** (1996) 1242
19. R. Wehlitz *et al.*, *Phys. Rev. Lett.* **67** (1991) 3764
20. G.H. Wannier, *Phys. Rev.* **90** (1953) 817
21. J.M. Feagin, *J. Phys.* **B28** (1995) 1495
22. J.M. Feagin, *J. Phys.* **B29** (1996) L1
23. M. Pont and R. Shakeshaft, *Phys. Rev. A*, to be published
24. R. Moshhammer *et al.*, *Nucl. Instrum. Methods* **B108** (1996) 425
25. M. Achler, dissertation, in progress, not published

Acknowledgement:

We would like to thank the following supporting organisations:

Alexander von Humboldt Stiftung, Willkomm Stiftung, DFG, BMBF, Graduiertenförderung des Landes Hessens, Studienstiftung des Deutschen Volkes, DOE, Division of Chemical Sciences, Office of Basic Energy Sciences, Office of Energy Research